

Acetophenone hydrogenation on polymer–palladium catalysts. The effect of polymer matrix

A. Drelinkiewicz^{a,*}, A. Waksmundzka^a, W. Makowski^a,
J.W. Sobczak^b, A. Król^a, and A. Zięba^a

^a Faculty of Chemistry, Jagiellonian University, 30-060 Kraków, ul. Ingardena 3, Poland

^b Institute of Physical Chemistry, Polish Academy of Science, 01-224 Warszawa, Kasprzaka 44-52, Poland

Received 10 June 2003; accepted 19 February 2004

Catalytic properties of Pd supported on two polymers of similar basicity but different electrical properties, a π -conjugated conducting-polypyrrole (PPY) and the electro-inactive poly(4-vinylpyridine) (PVP) have been studied in the hydrogenation of acetophenone (ACT) and compared with that of γ -Al₂O₃ supported Pd. Experimental evidences provided by several techniques: X-ray photoelectron spectroscopy (XPS), scanning (SEM) and transmission electron (TEM) microscopy, X-ray diffraction (XRD) and temperature programmed desorption (TPD) of hydrogen show that both polymers PVP and PPY exhibited ability to stabilize finely dispersed palladium nanoparticles, better this ability is offered by electro-inactive PVP. Palladium nanoparticles within a narrow range of size 2–20 nm as well as very high surface concentration of Pd (22.2 at %) in agglomerates were established in the latter polymer supported catalysts. Distinctly lower surface concentration of Pd (1.8 at %) and crystalline Pd particles of dimension within a wide range, from 5 nm up to ca. 1500 nm appeared in the matrix of electroactive polymer – PPY. The hydrogenation of ACT to ethylbenzene (ETB) via 1-phenylethanol (ACP) (as the intermediate) proceeded over all studied catalysts. The effects of solvents, Pd content, ACT concentration and the additives of ACP, ETB were also studied. The catalytic properties of Pd/PPY in terms of activity and selectivity significantly differ from those of Pd/PVP and Pd/Al₂O₃. Both latter catalysts offered high activity and selectivity in the C=O in ACT to C–OH reduction. Definitely lower activity and higher tendency towards the hydrogenolysis of C–OH in ACP reflected Pd/PPY catalysts. Such unprofitable properties of Pd/PPY can be attributed to relatively strong adsorption of all organic reactant ACT, ACP, ETB. A competition of the ACP and ETB with the ACT occurred only in the case of Pdcentres created in the electroactive polymer, whereas Pd sites dispersed in the electro-inactive PVP similarly as the ones in Al₂O₃ exhibited definitely more substrate – ACT specific character.

KEY WORDS: polypyrrole; poly(4-vinylpyridine); hydrogenation; acetophenone.

1. Introduction

Hydrogenation of carbonyl compounds is of great importance and hydrogenation of acetophenone (ACT) is a typical example of this category. The latter process is of industrial relevance because its intermediates and products are used in the pharmaceutical and cosmetic industry. Pt, Pd and Rh catalysts supported on conventional inorganic carriers Al₂O₃, SiO₂, TiO₂ [1–19] have already been studied in this reaction which was carried out either as liquid or gas-phase operations. The reaction network on Pt [2–7] and Rh [8–12] catalysts can be very complex, due to the possibility of the formation of several products. It has also been shown that in the hydrogenation of CO as well as carbonyl groups in crotylaldehyde and ACT the excellent activity offered Pt/TiO₂ catalysts due to metal–support interactions (MSI) induced in these systems [4,6,7]. Such interactions resulted in active sites that can selectively activate the carbonyl bonds towards hydrogen. They can be created in certain metal–support systems, particularly those using a reducible oxide like titania [6]. Only a consecutive reaction path comprising the hydrogenation of ACT to

ethylbenzene (ETB) via 1-phenylethanol (ACP) as the intermediate has been reported on Pd catalysts [15–19]. Various factors, among them the additives of acids into the reaction medium have been reported [13] as favouring the hydrogenolytic reaction. Present work aims to investigate the hydrogenation of ACT on polymer supported Pd catalysts and compare their performance with that of γ -Al₂O₃ supported Pd. Two polymers, the electroactive one – polypyrrole (PPY) and electro-inactive – poly(4-vinylpyridine) (PVP) were used. Recently, many researchers have focused studies on applying polymers as the matrices for dispersing metallic centres Pt, Pd. Specific properties of polymers among which their ability for the stabilization of finely dispersed metallic nanoparticles, swelling of polymer matrix and changing reactivity of catalysts due to various hydrophobic/hydrophilic character make polymeric carriers very attractive as potential supporting materials. The interesting and advantageous role of polymers in number of catalytic reactions have been reported in an excellent review paper [20] as well as in the recently published special issue of J. Mol. Catal. A [21].

It should be pointed out, that in full understanding of the catalytic behaviour of polymer-based catalysts is of

*To whom correspondence should be addressed.

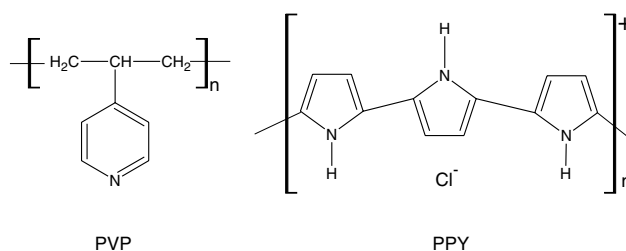
great importance not only of the detailed knowledge of active metallic centres but also the texture of polymeric support in its working state – during the catalytic reaction [22]. Information on the polymer-based catalysts in their dry state is only seldom relevant to their properties in the working state, i.e. the swollen state affected by the solvents used in the catalytic experiment. Swelling effectively separates the polymeric chains and therefore enhances dramatically the accessibility of the inner part of the polymer agglomerates. Swelling results in the formation of nanoporosity and it can make a substantial fraction of the “new” surface available for interactions with molecular species migrating through the polymer. Thus, in addition to macroporosity, the polymer-based catalyst possess also swelling-dependent nanoporosity, that depends on the degree of crosslinking of the polymer, the nature of catalytic reaction medium and its part in the catalytic process. The analysis of available literature information shows that the catalytic performance of polymer supported metals (Rh, Pd, Pt) depends critically on both the nanoenvironment surrounding the active centres as well as their accessibility. The latter is dramatically affected by the extent of swelling of the polymer matrix in contact with the reaction medium [23–26]. It has already been reported for a number of polymer-based catalysts that the active centres become accessible only when after contacting with a liquid medium, a swelling of the polymer matrix results in its nanoporosity. However, the relationship between catalyst performance and textural properties of the polymeric support in its working state only very few studies have been reported [26–28]. It should be pointed out, that the major objective of the present work was not to investigate the relationship between catalyst performance and textural properties of polymeric supports but to examine the reactivity of active sites created in the electroactive – PPY and electro-inactive – PVP matrices.

Metallic particles (Pt, Pd, Ag, Cu) electrochemically deposited on the thin film of various electroactive polymers have also been used as the electrodes in electrocatalytic oxidation of various organic molecules [29–32]. While metallic particles–conducting matrices systems seem also attractive from the catalytic point of view, this problem has not been studied as extensively as the electrocatalytic processes. Heterogeneous catalysts prepared by incorporation of Pd or Pt into powdered polyaniline (PANI) and PPY have been tested in the reduction of dissolved oxygen in water [33], hydrogenation of nitrobenzene to aniline [33,34] unsaturated $C \equiv C$ bonds in hexyne [35] and quinone systems [36]. The role of electroactive matrix in the catalytic reactivity of metallic centres has never been studied, and that is why the present investigations have been undertaken. These are mainly focused on the catalytic properties of Pd – PPY system.

PPY is a weak base ($pK = 10^{-10}$ [37]) and the most significant feature of this polymer is the ease of oxidation. Partial oxidation of polymer occurring

during the polymerization resulted in the delocalized positive charge compensated by insertion of anions, Cl^- in the present, starting PPY sample (Scheme 1). On reacting the PPY powder with $PdCl_2$ solution also oxidation–reduction mechanism was established resulting in a partial reduction of palladium ions and insertion of both Pd^{2+} and metallic Pd into the electroactive matrix [33,34,38]. As electro-inactive polymer, poly(4-vinylpyridine) (PVP) (scheme 1) was chosen because of the similarity in its physicochemical properties (specific surface area, the spherical shape of grains, basic properties $pK = 1.12 \times 10^{-4}$ [39]) to those of PPY. PVP – $PdCl_2$ complexes which were precipitated then mixed ethanol solutions of $PdCl_2$ and PVP effectively acted in the hydrogenation of unsaturated aldehydes and alcohols [23,24]. However, because of the location of Pd centres mainly inside the polymer matrix, their accessibility for the reactant was difficult and the activity of $PdCl_2$ – PVP system was to some extent determined by the ability of polymer to swell in the reaction medium [23,24]. Another preparation procedure of Pd/PVP was used in the present work. This procedure involved incorporation of palladium onto the powder of PVP (commercial reagent). Hydrolysis of palladium compounds that occurred due to alkaline properties of PVP resulted in the precipitation of palladium mainly onto the outer surface of polymer agglomerates [36].

The number of techniques (SEM, TEM, XRD, XPS, TPD) used in the present work allowed to characterize Pd species created in the Pd/PVP and Pd/PPY powders. The catalytic tests of ACT hydrogenation were performed in a liquid phase over a wide range of operating conditions. The effect of solvents, Pd content, concentration of ACT and the additives of hydrogenation products ACP, ETB were studied. In view of the physicochemical and catalytic results, an unprofitable role of electroactive polymer on performance of Pd/PPY was established. Such a role was manifested in the Pd crystallites of size within a wide range (5–1500 nm) as well as in the very low surface concentration of Pd on agglomerates of electroactive polymer. On the other side, the use of electro-inactive polymer – PVP and the same procedure of Pd insertion resulted in Pd/PVP catalysts of very similar properties to those of alumina supported Pd. Both latter Pd/PVP and Pd/ Al_2O_3 offered



Scheme 1.

much higher activity and selectivity in the ACT hydrogenation than that of electroactive-polymer supported Pd.

2. Experimental

2.1. Preparation of catalysts

PPY (BET surface area $7 \text{ m}^2/\text{g}$) was synthesized by polymerization of pyrrole at 0°C using HCl and $(\text{NH}_4)_2\text{S}_2\text{O}_8$ as the oxidant [38]. Poly(4-vinylpyridine) ($17 \text{ m}^2/\text{g}$) and $\gamma\text{-Al}_2\text{O}_3$ ($155 \text{ m}^2/\text{g}$) supports were commercial reagents (Aldrich).

Na_2PdCl_4 solution of NaCl : PdCl_2 molar ratio equal to 2.5–3 (PdCl_2 concentration $2.23 \times 10^{-3} \text{ mol}/\text{dm}^3$) was used as the precursor of palladium ions. Pd/PPY catalysts were prepared by exposure of polymer powder into the appropriate volume of Na_2PdCl_4 solution to obtain 1–5 wt% of Pd in the final catalyst. The suspension was stirred at room temperature when all of Pd complex had reacted with the polymer. This happened in ca. 30–60 min depending on the content of introduced Pd. The product was filtered off, washed with deionized water to eliminate Cl^- ions and then dried for 4 h at 60°C . The same PdCl_2 solution was used to prepare 4% Pd/PVP catalyst. The uptake of palladium by PVP powder occurred very slowly and it was complete after ca. 24 h of mixing a suspension of polymer in the Na_2PdCl_4 solution.

Pd/ Al_2O_3 4% was synthesized by the precipitation of hydrated palladium oxide onto alumina (spherically shaped grains of diameter ca. $100 \mu\text{m}$, BET surface area $155 \text{ m}^2/\text{g}$). Alumina dried for 16 h at 120°C was impregnated with Na_2PdCl_4 solution and subsequently treated with $0.1 \text{ mol}/\text{dm}^3$ NaOH solution. The catalysts were activated with hydrogen *in situ* immediately before the catalytic test (see section 2.3).

2.2. Characterization of catalysts

Characterization of Pd species with XRD, SEM, TEM, XPS techniques was performed for the catalysts activated with hydrogen using procedure described in Section 2.3. Catalytic experiments.

Colorimetric method based on the reaction between Pd^{2+} ions and thiourea was used to determine the content of Pd^{2+} in the catalysts. This method has been successfully applied to Pd – polyaniline [40]. In a typical procedure, the samples were treated with the excess of 5% thiourea solution in 0.05 M HCl and the concentration of extracted Pd^{2+} ions complexed with thiourea was determined colorimetrically after calibration. The content of Pd^0 was calculated as the difference between Pd introduced and Pd^{2+} extracted. The analysis was performed for the as-prepared Pd/PPY, the catalysts reduced only *in situ* with hydrogen (changing temperature $18\text{--}53^\circ\text{C}$ and time of catalysts reduction 30–120 min) prior the catalytic run and the catalysts taken from the reactor after the hydrogenation test (table 1).

X-ray diffraction studies (XRD) were carried out using a HZG-4 diffractometer with Cu $K\alpha$ radiation. Scanning electron microscopic investigations (SEM) were performed using a Philips XL-30 electron microscope. It was equipped with an X-ray microprobe which provided Pd distribution maps. The dispersion of Pd was characterized by transmission electron microscopy (TEM) using a Philips CM-20 instrument operated at 200 kV. Samples for TEM were prepared by placing a drop of the suspension of sample in ethanol onto a carbon-coated copper grid, followed by evaporating the solvent. The size of Pd particles was calculated by examination of over 100 particles in the TEM images at 66,000 magnification.

X-ray photoelectron measurements (XPS) were carried out *in situ* (without contacting the hydrogen activated sample with air) using a VG ES-CALAB 210 spectrometer with Al $K\alpha$ radiation (1254.6 eV , 10 kV). The binding energies (BE) were referred to the C 1s carbon peak at 284.7 eV . The C 1s, N 1s, O 1s, Cl 2p and Pd 3d core-level spectra were recorded.

Temperature-programmed desorption of hydrogen (TPD H_2) was performed in a classical experimental setup, equipped with a flow microreactor and a TCD detector (Valco). Prior the experiment the sample (20 mg) was reduced in a stream of H_2/Ar mixture (5% H_2 , Linde), in a temperature ramp of $10 \text{ K}/\text{min}$, up to 300°C in the case of 4% Pd/ Al_2O_3 . For the other catalysts lower upper temperature limit was used

Table 1
Colorimetrically determined contents of Pd^{2+} and Pd^0 (wt%) in the as-prepared and hydrogen activated catalysts

Catalyst	Initial Pd^0	Catalyst Pd^{2+}	$> \text{F}^0$ (%)	Reduction temperature ($^\circ\text{C}$)	Reduced Pd^0	Catalyst Pd^{2+}	F (%)
2% Pd/PPY	1.25	0.75	62	33	1.41	0.59	70.5
3% Pd/PPY	2.08	0.92	69	33	2.33	0.67	77.6
4% Pd/PPY	2.92	1.08	73	25	3.11	0.89	78.2
4% Pd/PPY				33	3.13	0.87	
4% Pd/PPY				43	2.99	1.01	
4% Pd/PPY				53	3.07	0.93	
5% Pd/PPY	3.42	1.58	68.4	33	3.45	1.55	69.0
4% Pd/PVP	–	4.00	–	33	1.45	2.55	36.2

(160 °C) due to low stability of the polymer supports. After reduction the sample was cooled in a flow of Ar to an ambient temperature. The adsorption of H₂ was performed by purging the microreactor with the H₂/Ar mixture. TPD of H₂ was measured using heating rate 10 K/min, in the same temperature ranges as during the reduction. Either pure Ar or the H₂/Ar mixture was used as a carrier gas, with the flow rate of 7.5 mL/min.

2.3. Catalytic experiments

Hydrogenation experiments were carried out in an agitated batch glass reactor at constant atmospheric pressure of hydrogen [36]. The solvents ethanol, 1-pentanol, 2-octanol and cyclohexane were used. The progress of the reaction was monitored by measuring the volume of hydrogen consumed as a function of reaction time (reproducibility of the method better than 5%). The following operating conditions were used: temperature 20–53 °C, catalyst concentration 0.04–0.15 g/10 cm³, initial ACT concentration (c_{ACT}^0) 0.043–0.43 mol/dm³. Before the hydrogenation experiment (in a typical procedure) the catalyst wetted with the solvent was activated *in situ* – inside the reactor by passing hydrogen through the reactor for 30 min, 15 min at 20 °C and 15 min at the temperature of reaction (33 °C in the standard procedure). Then, ACT solution was introduced and the hydrogenation test was started. Samples of liquids were withdrawn from the reactor via a sampling tube at appropriate intervals of time and analysed by gas chromatography (Auto System GCMS, Perkin-Elmer) with He as a carrier gas (flow rate 1 mL/min) and MS detector. Product separation was performed on a 30 m PE–5 MS 0.25 mm capillary column with a 0.25 µm coating, a temperature ramp 10 °C/min from 60° to 200 °C, injector temperature 200 °C.

Typically the hydrogenation experiment was carried out at 33 °C using 10 cm³ of ACT solution in ethanol ($c_{\text{ACT}}^0 = 0.086$ mol/dm³) and 0.04 g of catalyst. At the end of a run the catalyst was separated by filtration. The content of Pd²⁺ was then colorimetrically determined (table 1). The same content of Pd²⁺ found in the separate samples of catalyst activated only with hydrogen *in situ* revealed that no further reduction of Pd²⁺ occurred during the hydrogenation run.

In all cases studied, except Pd/PPY catalysts, the rate of hydrogen uptake was constant through at least the first 80% of the reaction. In the case of Pd/PPY such a constant rate was preceded by the induction period in which a slow increase in the rate occurred. The activity of catalyst was calculated from the linear part of the hydrogen consumption curves (induction period was omitted) and was referred to the 1 g of Pd in the catalysts (mol H₂/min g Pd). The rates of hydrogen consumption are reproducible to less than ca. 5% error in all systems. The hydrogenation of pure intermediate

i.e. ACP was also performed in standard conditions ($c_{\text{ACP}}^0 = 0.086$ mol/dm³, ethanol solvent, 33 °C). Blank experiments indicated a lack of activity in the absence of metal phase, in the presence of the pure PPY and PVP supports. No appreciable adsorption of the reactants ACT, ACP and ETB was observed on the pure polymers.

3. Results and discussion

3.1. Characterization of Pd species in the catalysts

3.1.1. Pd/PPY catalysts

Reaction of the PPY powder with Na₂PdCl₄ solution resulted in a partial reduction of palladium ions. As the data of colorimetric analysis show (table 1) 62–73% of the introduced palladium was metallic Pd. These findings are consistent with the XRD diffraction pattern in figure 1. The broad diffraction peaks centred at 2θ around 25° related to the PPY matrix and the very distinct peaks at 2θ = 40.1° and 46.6° characteristic of crystalline Pd are clearly visible. Only small increase in the content of zero-valent Pd occurred on activation with hydrogen (*in situ* prior the catalytic test). Hence, metallic palladium in the Pd/PPY was produced mainly due to the reducing properties of electroactive polymer, while the contribution of Pd⁰ produced under activation with hydrogen was distinctly lower. In consequence, Pd/PPY catalysts contained either unreduced Pd²⁺ ions and metallic Pd⁰ established also by the XPS Pd 3d spectra. The Pd 3d signal in the spectrum of hydrogen-activated 4% Pd/PPY consists of three peak components at BE equal to 335.03, 337.18 and 338.83 eV. They arise from metallic Pd, palladium bonded with chlorine and palladium most probably coordinated to

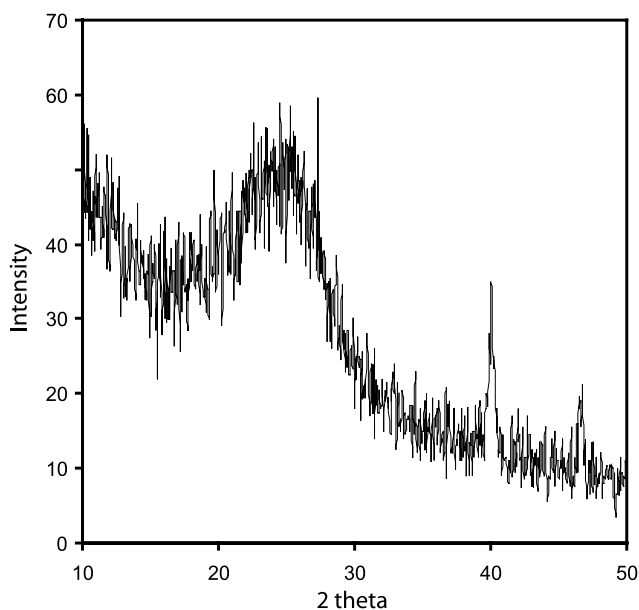


Figure 1. XRD diffraction of the as-prepared 2% Pd/PPY catalyst.

pyrrole rings, respectively. The first energy is identical as the one characteristic of the Pd-metal thus confirming the crystalline palladium in the Pd/PPY. However, the contribution of metallic Pd component is as low as only 8.6% whereas the peaks component attributed to palladium ions (91.4% in the whole palladium, table 2) evidently predominated. XPS – the surface sensitive technique shows the surface concentration of palladium as low as only 1.8 at % (table 3).

This finding is in disagreement with the result of colorimetric analysis showing metallic palladium as dominating in the electroactive matrices. Domination of metallic palladium was also confirmed by the EXAFS analysis. The EXAFS profile of Pd/PPY almost identical as the one of Pd-foil was obtained. The peak at Pd–Pd distances identical to that in the palladium foil evidently predominated in the Pd/PPY with a very small contribution of two peaks at the distances characteristic of Pd–Cl and Pd–N. However, taking into account complexity of the EXAFS data, the exact interpretation of these results will be separately published. Hence, such a difference in the content of metallic palladium may arise from the enhanced sensitivity of the XPS technique to the surface whereas the colorimetric and EXAFS techniques both provided data from the whole volume of the sample. The non-homogeneous distribution of metallic palladium through the agglomerates of PPY can be therefore postulated with the preferential location of metallic Pd inside the electroactive matrix.

Characterization of metallic phase in the hydrogen-activated Pd/PPY was performed with scanning and transmission electron microscopy (figures. 2 and 3). The SEM micrograph shows morphology of polymer typical of those reported in the literature [37]. Non-regular agglomerates of PPY composed of several small overlapping hemispheres of very similar diameter ca. 0.1–1 μm in size appeared. A few occasionally distributed, isolated, irregularly shaped white spots on this

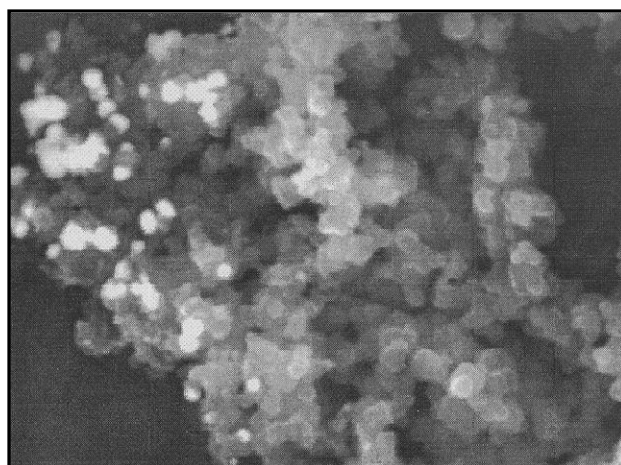


Figure 2. SEM micrograph of the hydrogen activated 4% Pd/PPY catalyst (magnification $\times 5000$).

SEM image (figure 2) of as large diameter as 300–1500 nm were identified by X-ray as Pd particles. However, also smaller Pd particles with diameter ranging from 5–40 nm were detected by the TEM (figure 3). The Pd size distribution diagram calculated from the TEM image (figure 3) shows similar contribution (15–20%) of particles 5–15 nm in size. Thus, the Pd particles of size within a wide range from the very small ones 5 nm up to as large as 1500 nm appeared in the electroactive matrix. Owing to a very wide range of the particle sizes, evaluation of an average diameter of Pd particles seems to be not very informative.

In the electrochemically deposited Cu, Pt, Pd–PPY, PANI nano-composites the metal particles with an average diameter of only few 1–5 nm were formed. The growth of such nanocomposites occurred directly on the electrode covered with a thin layer of polymer [30–32, 41]. Pd inclusions with a narrow dispersion (3–5 nm) were also obtained by electrochemical deposition of

Table 2
XPS data of Pd 3d_{5/2} in the hydrogen activated (at 33 °C) catalysts

Catalysts	Pd ²⁺		Pd ⁰ _{clusters}		Pd ⁰ _{metal}	
	BE (eV)	Share (%)	BE (eV)	Share (%)	BE (eV)	Share (%)
4% Pd/PPY	338.83	15.3	337.18	76.1	335.03	8.6
4% Pd/PVP	337.51	26.4	335.76	69.8	333.98	3.8

Table 3
Surface composition (in at %) characterized by XPS

Catalyst	C	O	Cl	N	Pd	C/N
PPY	67.70	13.02	2.36	16.92	–	4.00
4% Pd/PPY	68.90	12.30	2.10	13.80	1.80	4.99
PVP	84.33	8.05	–	7.62	–	11.07
4% Pd/PVP	25.7	47.6	2.50	2.00	22.20	12.85

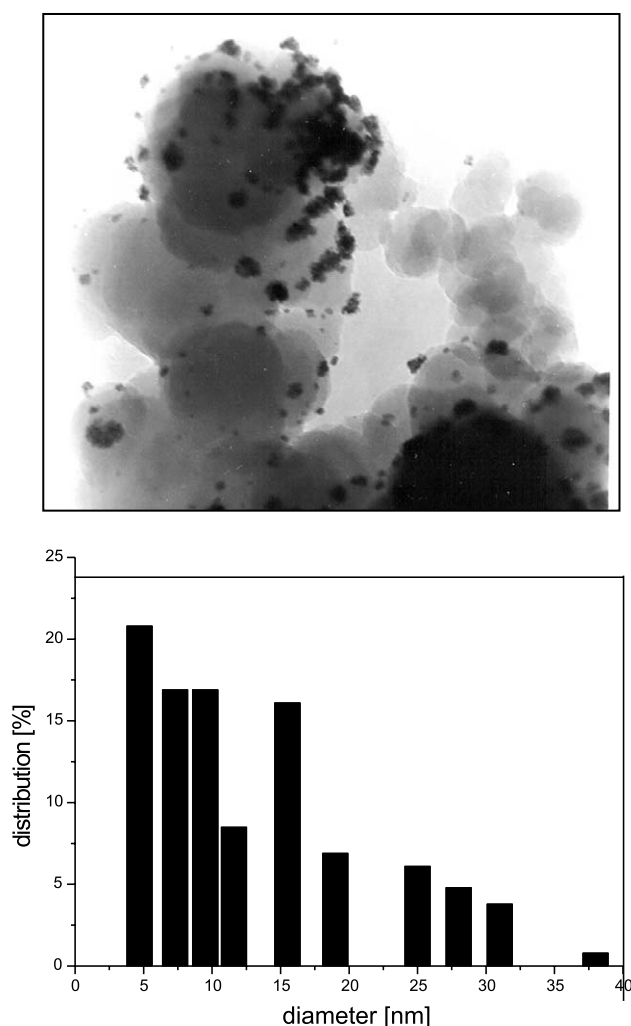


Figure 3. TEM micrograph of the hydrogen activated 4% Pd/PPY catalyst (magnification $\times 66,000$) and the Pd size distribution diagram.

pre-formed Pd-nanoclusters onto the thin PPY film [42]. It should be pointed out, that in the electrochemically synthesised nano-composites films the loading of metal is usually very low.

Much higher Pd loading introduced into powdered polymer such as in the present 1–5% Pd/PPY catalysts resulted however, in the Pd crystallites of size within wide range. Nanoparticles 5 nm in size as well as the large ones of diameters (ca. 1000–1500 nm) comparable to those of pure polymer agglomerates were then produced.

3.1.2. Pd/PVP catalysts

Activation of Pd/PVP catalysts with hydrogen resulted in a partial reduction of palladium ions revealed by colorimetric (table 1) and XPS analyses (table 2). Three energy states of palladium at 337.51, 335.76 and 333.98 eV were found in the Pd (3d) XPS spectrum (table 2). The first energy was assigned to Pd^{2+} bonded with Cl, the last 333.98 eV to the metallic

palladium. The energy 335.76 eV which is lower than that of metallic Pd is often attributed to electron deficient $\text{Pd}^{\sigma+}$ or to Pd clusters [24]. The latter Pd species were found by XPS as the dominating (69.8%) state of palladium within the surface of hydrogen-activated Pd/PVP catalyst (table 2). Indeed, the XRD diffraction confirmed highly dispersed Pd in the PVP matrix because only a small broadening on the base line in the diffraction region characteristic of crystalline Pd was observed. It is more interesting to observe that at the same loading of Pd (4%) in both PVP and PPY polymers, the surface concentration of Pd (22.2 at% of Pd) in the electro-inactive PVP is ca. 12 times higher than the 1.8 at% in the Pd/PPY (table 3). The morphology of PVP agglomerates similar to that of PPY can be seen on the SEM image of 4% Pd/PVP catalysts (figure 4). Polymer agglomerates (4–10 μm) are composed of less or more spherical grains with diameters slightly higher compared with those of PPY. High ability of PVP to stabilise well dispersed metallic Pd resulted in a very homogeneous distribution of Pd element through the polymer, established by the X-ray map [36]. TEM image of the hydrogen-activated 4% Pd/PVP shows irregularly shaped black areas of diameter within narrow range 2–20 nm (figure 5). The size distribution diagram (figure 5) estimated from the TEM results shows the domination of the particles 5 nm in size.

Hence, in contrary to the Pd/PPY, only the nanoparticles of Pd with a homogeneous size distribution appeared in the Pd/PVP. Such effect revealed better stabilising properties of PVP by preventing the aggregation of Pd to the large crystalline particles observed in the case of electroactive matrix. This ability makes PVP attractive as a potential supporting material for palladium catalysts.

3.2. Temperature programmed desorption of hydrogen

The properties of Pd centres existing in the dry powders of electroactive and electro-inactive polymers were characterized with the TPD of hydrogen and compared with those of 4% Pd/ Al_2O_3 (figure 6). These measurements can provide information about the strength of interaction of hydrogen with the Pd sites in catalyst. It is well known that the peak position and shape are strongly influenced by experimental parameters such as the carrier flow rate, heating rate, transport limitation and readsorption effects. The experiments performed were selected to obtain reproducible data with high signal to noise ratio, as well as to eliminate diffusion effects [43]. However, no systematic studies of these effects were performed. In the TPD profiles measured using H_2/Ar mixture (figure 6a) for both polymer-based catalysts (4% Pd/PVP and 4% Pd/PPY) two peaks are clearly seen: the distinct one at around 60 $^\circ\text{C}$ and second-less intensive but much broader at

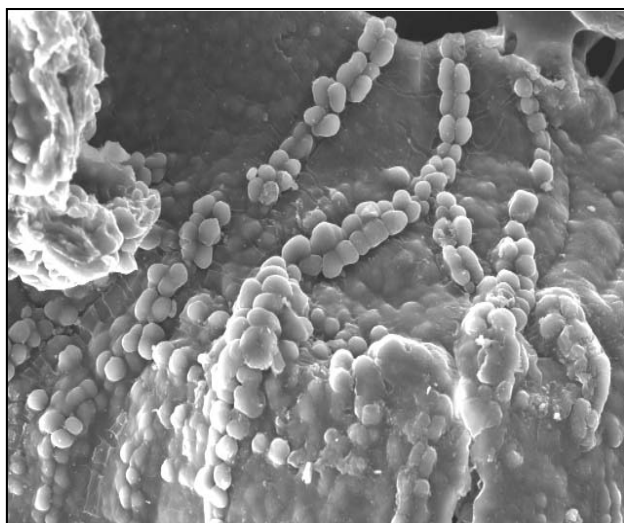


Figure 4. SEM micrograph of the hydrogen activated 4% Pd/PVP catalyst (magnification $\times 500$).

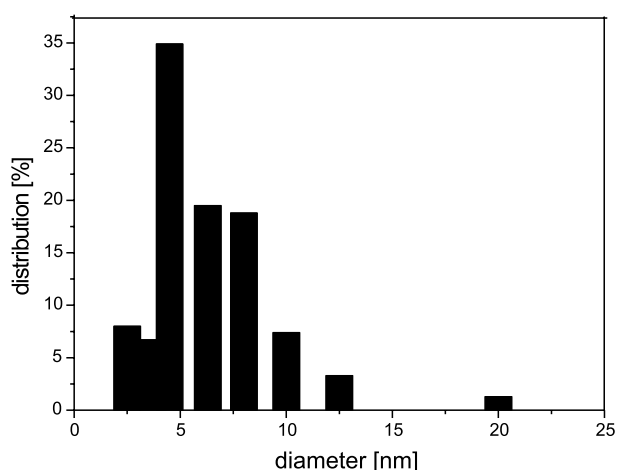


Figure 5. TEM micrograph of the hydrogen activated 4% Pd/PVP catalyst (magnification $\times 66,000$) and the Pd size distribution diagram.

higher temperatures. The low temperature peaks (at 60 °C) are assigned to hydrogen derived from the decomposition of β -palladium hydride, the second may

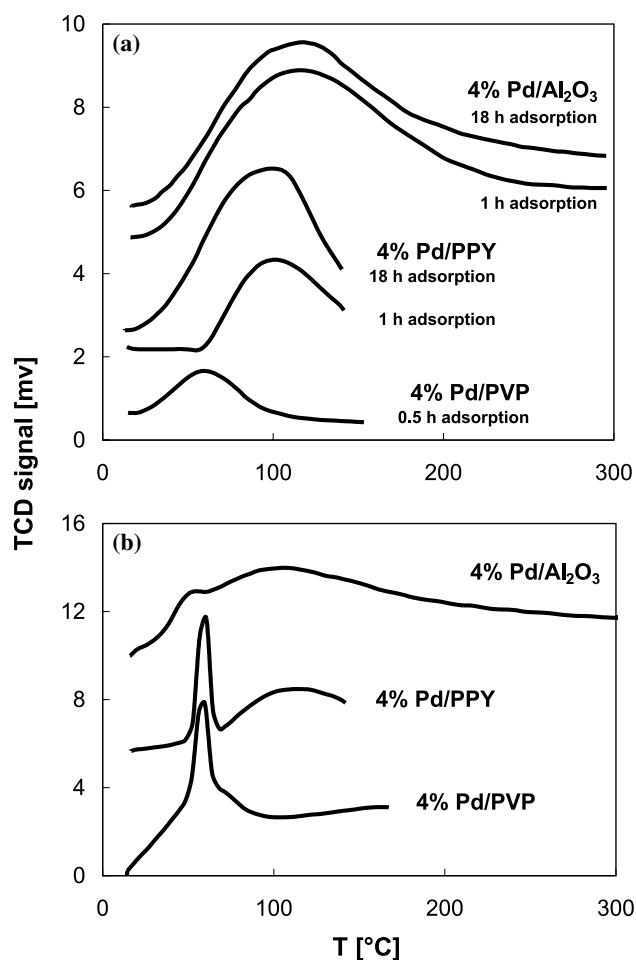


Figure 6. TPD profiles of hydrogen: (a) flowing gas a mixture 5% H₂-Ar; (b) flowing gas pure Ar.

be attributed to the chemisorbed hydrogen. In the TPD profile of electro-inactive Pd/PVP the low temperature peak dominates whereas only a very weak shoulder at slightly higher temperature attributed to chemisorbed hydrogen appeared. On the other hand, in the TPD profile of 4% Pd/PPY similarly as in 4% Pd/Al₂O₃ very broad peaks of chemisorbed hydrogen located at distinctly higher temperatures are seen. The difference between individual catalysts with respect to the chemisorbed hydrogen is better recognised in the TPD profile obtained in pure Ar as a carrier gas (figure 6b). Only a single, broad maximum resulting from desorption of the chemisorbed hydrogen is then observed. The much higher capacity of hydrogen as well as distinctly higher temperature of H₂ desorption is observed for the 4% Pd/PPY comparing with that of 4 % Pd/PVP. Actual content of the exposed Pd in 4% Pd/PVP may be higher than represented by the peak area in figure 6 b since the coverage might be not complete due to relatively high temperature of adsorption.

Formation of the palladium hydride phase requires relatively large crystallites of Pd, whereas chemisorption of hydrogen atoms should be related to small Pd

particles. The TPD results indicate that only in the 4% Pd/Al₂O₃ small Pd particles predominate, since formation of β -PdH_x is negligible, while both polymer-based catalysts contain large Pd particles responsible for β -PdH_x formation, as well as small exposed metal particles containing hydrogen chemisorption sites. According to [44] small Pd crystallites chemisorb H atoms more strongly and in consequence more dispersed sample will have a higher H₂ desorption temperature. Higher H₂ desorption temperature is observed for Pd/PPY in which besides the Pd crystallites of relatively large size (figure 2) the smaller ones are also present (figure 3) that are responsible for relatively strong chemisorption of hydrogen.

More chemisorbed hydrogen was observed for Pd/PPY after prolongation of the adsorption time. This effect may result from limited diffusion rate of H₂ molecules through the polymer. Longer adsorption time would be necessary for the complete saturation of the adsorption sites on Pd particles located inside the polymer matrix. No such effect was observed for the catalyst containing a typical porous support (4% Pd/Al₂O₃). Another possible explanation of this effect – incomplete reduction of Pd ions before adsorption of H₂ – is less likely. The initial reduction degree of Pd²⁺ ions in the as-synthesised 4% Pd/PPY was high (73%, table 1) as well as before the TPD measurements the sample was additionally reduced in flow of 5% H₂/Ar at 160 °C.

3.3. Hydrogenation experiments

In agreement with the finding for Pd catalysts [15–18] the hydrogenation of ACT to ETB via 1-phenylethanol (ACP) occurred over all PPY, PVP and alumina supported Pd. ACP and ETB were identified by gas chromatography–mass spectrometry (GCMS) analysis as the only products formed in the present studies. Thus, active sites created in both PPY and PVP polymers are able to hydrogenate carbonyl groups C=O to the alcohol C-OH ones and to transform the latter to >CH₂.

3.3.1. The effect of solvent

Hydrogenation experiments were performed to examine the role of solvents in the activity of studied

catalysts. In the case of polymer-based catalysts this role may be connected not only with the solubility of hydrogen and solvent polarity but also with the swelling ability to various extent in the solvent medium. The results are collected in table 4. It can be seen that the solvent polarity [dielectric constant (ϵ)] more than the solubility of hydrogen in the solvents affect the activity. In agreement to the findings on Pd/AlPO₄ [17] the activity of our Pd/Al₂O₃ is high in ethanol and 1-pentanol, but it decreases in solvents of lower ϵ . Other effects can be seen on polymer-based catalysts. The activity of Pd/PVP is much higher in the polar solvents than in the cyclohexane. In 1-pentanol and ethanol this activity is comparable to that of Pd/Al₂O₃ but is around two times higher in the 2-octanol solution. The observed high activity in alcohol solvents could easily be due to swelling of PVP to various extents occurring in polar medium [23,24]. Pd/PPY exhibited very low activity in all solvents except ethanol. Activity in ethanol was more than 10–20 times higher than in the remained less polar solvents. Thus, ethanol was chosen as the solvent in all subsequent catalytic experiments performed in the present work. The nature of solvent was also found to affect the activity of Pd/PPY in the nitrobenzene hydrogenation [34]. The better activity similarly as in the present studies was obtained in ethanol solvent. It is very probable that ethanol as the most polar among the solvents used in the present work, exhibited a satisfactory high solvating properties with respect to ACT molecule, thus hindering its adsorption on the Pd sites existing in the electroactive matrix. The results in table 4 enable also to compare the activity of individual catalysts. In all studied solvents the activities of Pd/PVP and Pd/Al₂O₃ are comparable, and all are much higher than those of electroactive matrix-PPY supported Pd. With the most active 4Pd/PVP catalysts (33 °C, 0.04 g catalyst in 10 cm³ of ethanol solution) a few experiments were carried out to attain sufficiently high agitation frequency at which the rate of hydrogen uptake did not depend of it. This agitation frequency was used in all the hydrogenation tests thus showing the absence of external gas–liquid mass transfer limitation under the standard hydrogenation conditions (ethanol, 33 °C) of the present work. The effect of 4% Pd/PVP catalyst concentration on the rate of hydrogen

Table 4
The effect of solvent on the initial activity [mol H₂/min g Pd $\times 10^{-3}$] of catalysts

Solvent	Dielectric constant	Solubility of H ₂ (mol/cm ³ 10 ⁻⁶) ^a	4% Pd/PPY	4% Pd/PVP	4% Pd/Al ₂ O ₃
Cyclohexane	2.02	3.97	Inactive	2.68	5.15
2-Octanol	8.13		0.35	21.56	9.31
1-Pentanol	15.1	1.52	0.17	10.68	12.87
Ethanol	25.3	3.40	3.72	14.50	12.44

^aSolubility of H₂ at 34 °C and p_{H_2} = 1 atm [45, 46].

uptake was studied in the range of 0.024–0.15 g/10 cm³ of ethanol solution at 33 °C. The rate of hydrogen uptake was found to increase by nearly four times, when the catalyst amount increased from 0.024 to 0.1 g/10 cm³ (figure 7) (0.04 g of catalyst was used in the standard hydrogenation procedure). The linear dependence of the initial rate with the catalyst concentration also proved the absence of external gas–liquid mass transfer limitation [10,47].

To determine apparent activation energy the hydrogenation tests were carried out with standard procedure ($c_{\text{ACT}}^0 = 0.086 \text{ mol/dm}^3$) at temperature 20–53 °C. In these experiments the catalysts were activated with hydrogen 15 min at room temperature and 15 min at the temperature of reaction. However as the data in table 1 show the temperature of Pd/PPY activation did not essentially affect the content of metallic Pd determined in the catalysts after the hydrogenation test. Maybe, because in the catalysts predominated zero-valent Pd formed during the palladium insertion, due to reducing properties of PPY. At higher temperatures, similarly as in the standard condition (33 °C) the rate of hydrogen uptake was practically constant up to ca. 80% of ACT conversion. Using such constant rates the Arrhenius plots (figure 8) were prepared. In the case of 4% Pd/PPY this plot is linear within the whole temperature range while for the much more active 4% Pd/PVP the linear relationship is seen only at lower temperatures. Activation energies for the reaction at 33 °C are calculated to be 8.1 kcal/mol on 4% Pd/PPY and 9.6 kcal/mol on 4% Pd/PVP. The obtained values are in agreement with the literature data 8–11 kcal/mol for the kinetically controlled ACT hydrogenation on Pt/SiO₂, Pt/Al₂O₃ and Pt/TiO₂ [4,5] as well as 10.5 kcal/mol on CuCr₂O₃ [14].

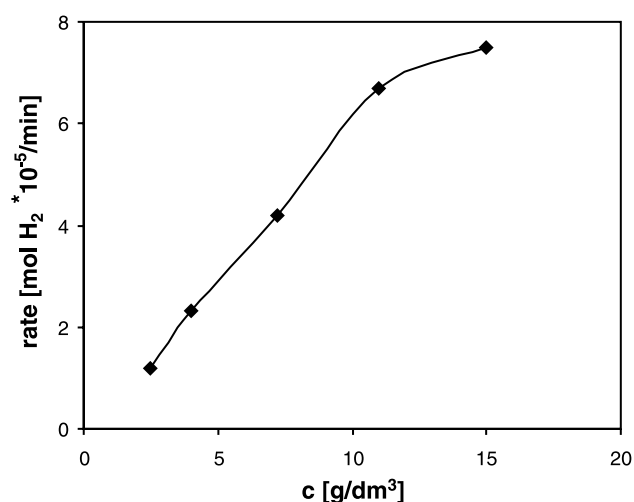


Figure 7. Initial rate of hydrogenation (mol H₂ × 10⁻⁵/min) as a function of 4% Pd/PVP concentration (ethanol, 33 °C, $c_{\text{ACT}}^0 = 0.086 \text{ mol/dm}^3$)

3.3.2. The effect of polymer

Typical hydrogen consumption curves [mol H₂ × 10⁻⁵] obtained in the hydrogenation carried out in ethanol solvent at 33 °C are compared in figure 9. The difference in the shape of curves on Pd/PPY (figure 9a) from those on Pd/PVP and Pd/Al₂O₃ (figure 9b) is seen, especially in the initial stage of the hydrogenation experiment. An induction period can be seen only on Pd/PPY, especially distinct for catalysts with low Pd content (2–3% Pd). When the content of Pd increased, the induction period become less and less distinct and completely vanished on catalyst with 5% Pd. The procedure of catalyst activation with hydrogen *in situ* has essential role on induction period. In particular the nature (composition) of liquid used to wetting the catalyst has a drastic effect.

Wetting of the catalyst with ethanol only under activation with hydrogen resulted in a relatively short induction period, while ACT-containing ethanol solution produced very long one with a consequent lowering of the catalyst activity. The effect of induction period has been reported by number of authors in the hydrogenation of various reactants. Most frequently it was correlated with enhanced chemisorption of the reactants. This seems also very probable in the present Pd/PPY catalysts, experimentally confirmed by examination of the products ACP and ETB additives on their activity (Section 3.3.4).

A break in the hydrogen uptake curves (figure 9) although not very distinct shows the ACT reduction in two stages differing in the rates, similarly as reported on Pd/C catalyst [15]. The hydrogenation of ACT to the alcohol (ACP) predominates in the first, whereas the second stage corresponds to the hydrogenolysis of ACP to ETB.

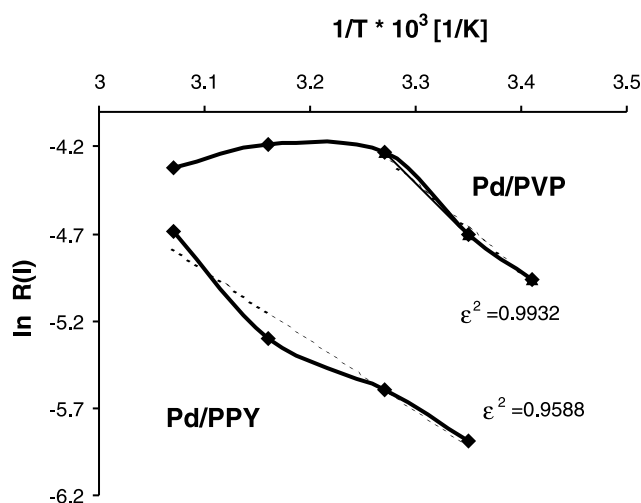


Figure 8. Arrhenius plots for the hydrogenation of ACT on 4% Pd/PPY (A) and 4% Pd/PVP (B) catalyst in the temperature range 20–53 °C (ethanol, catalyst concentration 4 g/dm³, $c_{\text{ACT}}^0 = 0.086 \text{ mol/dm}^3$).

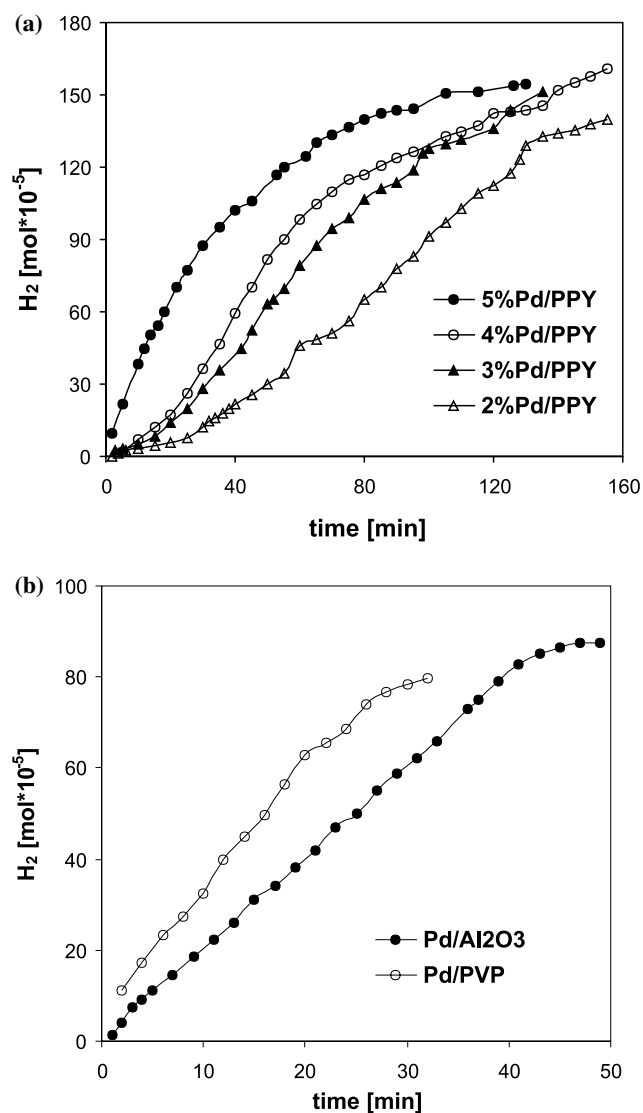


Figure 9. Hydrogen consumption curves in the hydrogenation of ACT: (a) Pd/PPY of various Pd loading; (b) 4% Pd/PVP and 4% Pd/Al₂O₃.

Thermodynamic data [14] show at hydrogen pressure 1 atm and temperature 298 K the free energy changes for the formation of ACP and ETB via the reactions $ACT + H_2 = ACP(I)$ and $ACP + H_2 = ETB = H_2O$ (2) as equal to -5.03 and -18.68 kcal/mol, respectively. The equilibrium constants are calculated to be 4.9×10^3 and 5.13×10^{13} for reactions 1 and 2, respectively. Thus, the extent of equilibrium conversions as high as 98.6% for ACT and 99.9% for ACP were calculated [14]. In view of above data ACT can be almost completely reacted to ACP as well as ACP to ETB in experimental conditions used in the present work.

The hydrogenation of $C=O$ proceeded with a constant rate of H_2 uptake (R, I) until more than 1 molar equivalent of hydrogen had been consumed and then slowed markedly (R, II). Thus, together with the $C=O$ to $C-OH$ hydrogenation the reduction of $C-OH$ to

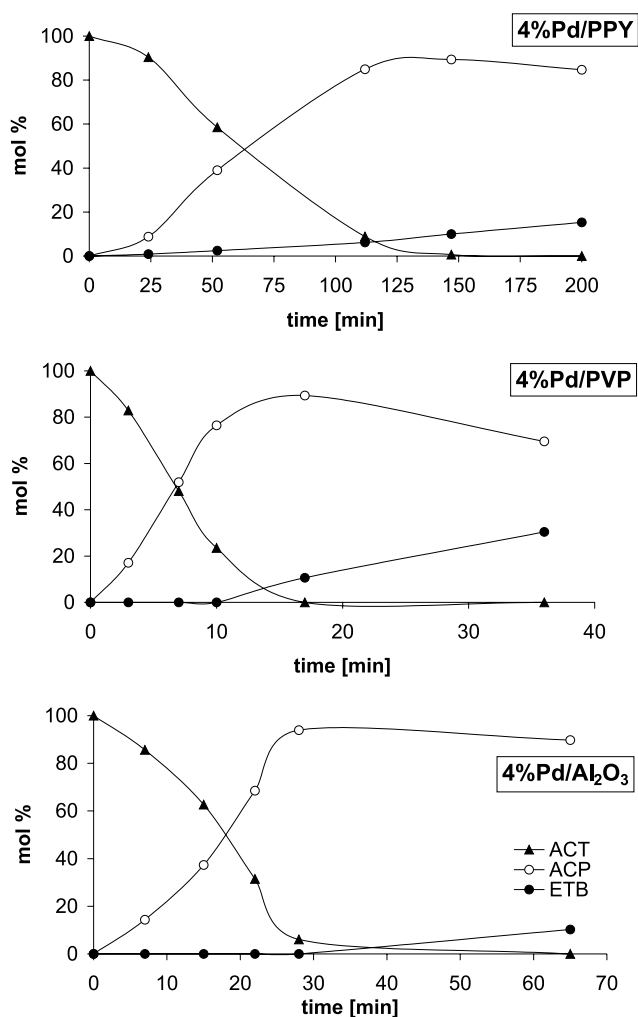


Figure 10. Change of reactants ACT, ACP and ETB concentration (mol%) as a function of reaction time (ethanol, 33 °C, $c_{ACT}^0 = 0.086$ mol/dm³).

CH₂ proceeded. The latter conclusion is confirmed by the plots of reagents concentrations versus the reaction time (figure 10). The concentration of ACT decreases while that of ACP increases and passes through the maximum. ETB is formed from the very beginning of the reaction on Pd/PPY only. On the other hand, on both Pd/PVP and Pd/Al₂O₃ similarly as reported on Pd/AlPO₄ [17], an appreciable amount of ETB is observed only when nearly all of the starting ACT is converted to ACP (figure 10), similarly as reported on Pd/AlPO₄ [17]. From this type of the reaction profile it was concluded [17] that ACT is more tightly adsorbed at active sites than is ACP. As long as the concentration of ACT is high enough, selective adsorption of this compound is predominant and only very low surface concentrations of the intermediate ACP exist. This concept is also true on Pd/Al₂O₃ and electro-inactive PVP supported Pd. The formation of ETB from the very beginning of the reaction on Pd/PPY demonstrates that the surface concentration of intermediate – ACP and/or the

Table 5

The influence of Pd content and the additives of ACP and ETB on the rate $[(\text{mol H}_2/\text{min g Pd}) \times 10^{-3}]$ of stage I (R, I) and stage II (R, II) in hydrogenation on Pd/PPY

Pd (wt%)	Exp. No	Initial concentration (mol/dm ³)			(R, I)	(R, II)	Decrease in the (R,I) (%)
		ACT	ACP	ETB			
2	A	0.086	–	–	3.73	2.01	
3	A	0.086	–	–	3.53	1.78	
	B	0.086	0.0055	–	2.60		26.3
	C	0.086	0.022	–	1.78		49.5
4	A	0.086	–	–	3.72	0.95	
		–	0.086	–	0.55		
	B	0.086	–	0.065	3.18	0.25	
5	A	0.086	–	–	3.23	0.60	
	B	0.086	0.022	–	2.78		13.9

intrinsic rate of the ACP hydrogenolysis is then higher.

The data in table 5 show practically the same rate of the first stage (R, I) independently of the Pd content in the Pd/PPY catalysts. On the other hand the increase in the content of Pd resulted in a slow decrease in the rate of the second stage (R, II) in which ACP was reduced to ETB. Simultaneously, breaks on the hydrogen uptake curves transform to larger amounts of hydrogen showing the increased contribution of the hydrogenolysis in the first stage of the process. As a very probable reason of a decreased rate in the second stage, the strong adsorption of the reaction products ACP, ETB can be considered.

3.3.3. The effect of ACT concentration

The effect of the initial ACT concentration (c_{ACT}^0) was studied at 33 °C and the relations between the rate of the first stage (R, I) and c_{ACT}^0 are presented in figure 11. The zero order of reaction towards ACT is observed within the whole range of c_{ACT}^0 on Pd/PVP and Pd/Al₂O₃ (figure 11b) similarly as reported on Pt and Pd catalysts [4,14,17]. Another effect of c_{ACT}^0 appeared on electroactive polymer supported Pd. The rate was found to be practically constant only within c_{ACT}^0 concentration as low as 0.043–0.086 mol/dm³ (figure 11a). The higher c_{ACT}^0 resulted in a very long induction period with consequent decrease in the rate of the ACT to ACP reduction (first stage). Although a long induction period makes difficult the exact calculation of the rate (very short linear part of the hydrogen consumption curves) an inhibitory effect of large ACT concentration appeared either at 2 and 4% of Pd in the electroactive matrix (figure 11a). A strong chemisorption of ACT molecules on Pd sites created in the electroactive matrix may be considered as a probable reason of such effect.

3.3.4. The effect of ACP and ETB additives

When ACP is added into the solution at the start of experiment, it has a marked retarding effect on the rate

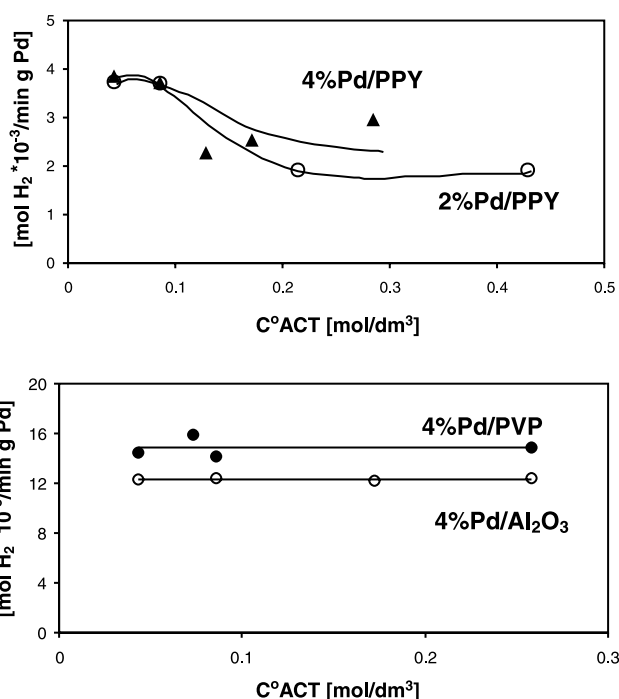


Figure 11. The influence of initial ACT concentration (c_{ACT}^0) on the rate in stage I (R, I).

of ACT reduction on Pd/PPY only, whereas it has no observable effect on the rate at which ACT reduces over Pd/PVP and Pd/Al₂O₃. As figure 12 shows the additives of ACP resulted in a distinct induction period as well as in the decrease in the activity of Pd/PPY. As the amount of introduced ACP is increased, the inhibitory effect becomes correspondingly more and more pronounced (table 5). As the same number of ACP moles are introduced, the inhibitory effect is more distinct on the catalyst with lower content of Pd. An inhibitory phenomenon also appears due to the ETB additives. ETB has no drastic effect on the rate at which C=O in ACT reduces to C-OH, but it causes almost complete retardation of the second stage in which ACP reduces to

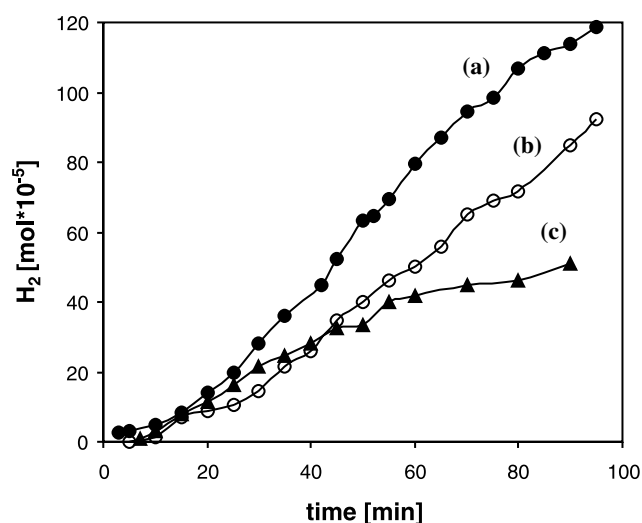


Figure 12. The effect of ACP additives on the course of ACT hydrogenation on 3%Pd/PPY at 33 °C. ACT the only reagent in the reactor $c_{\text{ACT}}^0 = 0.086 \text{ mol/dm}^3$ (A), 0.086 mol/dm^3 of ACT and 0.0055 mol/dm^3 of added ACP (B), 0.086 mol/dm^3 of ACT and 0.022 mol/dm^3 of added ACP (C).

ETB. Identical inhibitory effect of propylbenzene in the hydrogenation of propiophenone (ethanol solvent) has been reported on Pd/C catalyst [15].

In the hydrogenation of the intermediate – ACP (in standard conditions) on 4% Pd/PPY as the only product ETB was formed. The rate of ACP reduction was ca. four times lower than that of ACT (table 5) in the same conditions. Hence, Pd/PPY exhibited much higher activity of carbonyl group C=O reduction compared with that of C-OH hydrogenolysis. The reduction of ACP occurred with almost constant rate up to ca. 25% of ACP conversion and then slowly decreased, most probably due to the increased content of ETB in the reaction medium. Such inhibition effect also existing in the course of ACP hydrogenation confirmed strong adsorption of the reaction product in the case of electroactive matrix supported Pd.

In conclusion, active sites created in the electroactive matrix differ from those in the alumina and electro-inactive polymer. The enhanced chemisorption of all the organic reactants ACT, ACP, ETB occurred on sites formed only in the electroactive polymer – PPY. Relatively strong chemisorption of the ACT molecules may be responsible for the induction period in the very beginning of the reaction as well as the lowering of Pd/PPY activity at higher initial ACT concentration. Strong chemisorption of reaction products ACP and ETB and their competition with the ACT molecules also resulted in lowering of Pd/PPY activity and in less selective C=O reduction. On the other hand, very similar temperatures of hydrogen desorption for Pd/PPY and Pd/Al₂O₃ (figure 6) may suggest comparable strength of hydrogen chemisorption in both catalysts.

Thus, unprofitable role of electroactive matrix can be related to the enhanced adsorption of organic reactants. It is difficult to decide if such role can be related to the structure of polymer itself leading to the interaction of pyrrole units with the organic reactants (ACT, ACP, ETB) thus making difficult access to the active centres inside the polymer agglomerates. However, the interactions between the metallic Pd and π -conjugated polymer may also modify reactivity of the Pd centres in a way of the enhanced adsorption of the organic reactants.

Recently, many researchers have focused their studies on the interactions between metallic particles and conductive polymers. The systems composed of the thin film of polymers with embedded metallic particles have been used in these studies in view of their potential application as the new electronic (semiconducting) devices. In this context the interactions at metal/polymer interfaces such as Al, Cr, V, Ag, Cu, Au – PPY and polythiophene were studied [30,41,48–50]. The general behaviour of metal/electroactive polymer contact can be considered as electronic in nature and can be predicted from the electronic properties: work function, energy of the valence and conducting bands of the particular reagents [48]. As expected the reactivity of individual metals differed from each other and most frequently this reactivity was considered in term of charge transfer affecting the π conjugation in the polymer matrix. However, to a best of our knowledge a detailed interactions in such systems particularly with respect to the metallic particles are not yet fully understood because most of studies was concentrated on the changes in electronic properties of polymer induced by metal atoms. Detailed explanation of a difference in the adsorption properties of the active sites created in the electroactive and electro-inactive polymers established in the present work seems therefore difficult. However, in view of the present observation it is evident that application of Pd/PPY as the heterogeneous catalysts in hydrogenation of carbonyl compounds did not provide satisfactory results.

It can not be excluded that applying catalysts similar to those used in the electrocatalytic processes—i.e. samples with the zero-valent Pd nanoparticles only, uniformly dispersed in the thin film of electroactive matrix – enable to recognise more evidently the role of electroactive polymer. This type of palladium catalyst containing silica grains coated with thin film of electroactive polymer–polyaniline have already been tested in our introductory catalytic experiments.

On the other hand, very promising catalysts were obtained using the electro-inactive polymer PVP. The profitable properties of Pd/PVP can be attributed to the preferential location of Pd nanoparticles onto the surface of the polymer agglomerates as well as to the character of Pd sites which were more substrate (ACT) specific than those in the electroactive matrix. All of these properties make Pd/PVP very attractive catalysts

and investigations are in progress for a better knowledge of these new catalysts.

4. Conclusions

The substantial difference between the reactivity of Pd active sites created in the electroactive PPY and the electro-inactive PVP polymers was established. The Pd crystallites of size within wide range 5 nm up to ca. 1500 nm appeared in the Pd/PPY, whereas owing to much higher stabilizing ability of PVP the finely dispersed Pd nanoparticles 2–20 nm in size were formed in the Pd/PVP catalyst. The hydrogenation of ACT to ethylbenzene (ETB) via 1-phenylethanol (ACP) as the intermediate occurred over all studied catalysts. The activity of electro-inactive polymer supported Pd was comparable to that of Pd/Al₂O₃ and both such catalysts offered much higher activities than that of Pd/PPY. Both Pd/PVP and Pd/Al₂O₃ reduced selectively C=O in ACT to C-OH. The zero order of reaction towards ACT concentration was established for Pd/PVP and Pd/Al₂O₃ catalysts. Their activities were found to retain unchanged under the additives of the reaction products ACP and ETB. Thus, no competitive adsorption of the reaction products and ACT occurred in these catalysts. On the other hand, strong competition of the reaction products ACP and ETB with the substrate ACT for the active sites created in the electroactive matrix resulted in distinctly lower activity of Pd/PPY as well as in less selective C=O reduction. A disadvantageous role of electroactive polymer on reactivity of Pd centres is therefore postulated. Such a role manifested in a very low surface concentration of zero-valent Pd in the PPY agglomerates as well as in an enhanced adsorption of all organic reactants (ACT, ACP, ETB) on the active sites created in the electroactive polymer. It can not be excluded that interactions between Pd particles and π -conjugated electroactive polymer may modify the reactivity of Pd centres in a way of the enhanced adsorption of the organic reactants, observed in the present investigations. On the other hand, the electro-inactive polymer PVP supported Pd seems a very promising system. Specific properties of polymer among which the high ability to stabilisation of finely dispersed Pd nanoparticles as well as location of Pd mainly onto the outer surface of polymer agglomerates make PVP attractive as a potential supporting material for the palladium catalysts.

Acknowledgments

The authors gratefully thank to Dr Magdalena Hasik for gift of polypyrrole sample. This work was partially supported by the Polish Committee for Scientific Research (KBN) grant number 3 T09A 004 16.

References

- [1] N.S. Barinov, E.G. Lebedeva and D.V. Mushenko, *Zh. Prikl. Khim.* 42 (1969) 2613.
- [2] P. Geneste and Y. Lozano, *C.R. Acad. Sc. Paris C* 280 (1975) 1137.
- [3] M. Freifelder, T. Anderson, Y.H. Ng and V. Papendick, *J. Pharm. Sci.* 53 (1964) 967.
- [4] S.D. Lin, D.K. Sanders and M. A. Vannice, *Appl. Catal. A; Gen* 113 (1994) 59.
- [5] S.D. Lin, D. K. Sanders and M. A. Vannice, *J. Catal.* 147 (1994) 370.
- [6] M.A. Vannice *Catal. Today* 12 (1992) 255.
- [7] M.A. Vannice, *Top. Catal.* 4 (1997) 241.
- [8] J. Bergault, M.V. Rajashekharam, R. V. Chadhari, D. Schweich and H. Delmas, *Chem. Eng. Sci.* 52 (1997) 4033.
- [9] I. Bergault, C. Joly-Vuillemin, P. Fouilloux and H. Delmas, *Catal. Today* 48 (1999) 161.
- [10] I. Bergault, P. Fouilloux, C.Joly-Vuillemin and H. Delmas, *J. Catal.* 175 (1998) 328.
- [11] L.H. Frejdlin, N.W. Borunowa, L.I. Gwinter, S.S. Danielowa and R.N. Badah, *Izv. Acad. Nauk. SSSR* (1970) 1797.
- [12] G.D. Zakumbajewa, L.A. Beketajeva, S.Z. Ajtmagambetova and W.F. Wozbizenski, *Zh. Prikl. Khim.* 8 (1989) 5.
- [13] J. Masson, P. Cividino and J. Court, *Appl. Catal. A : Gen.* 161 (1997) 191.
- [14] G. Csomontanyl, M. Netta and M. Balmez, *Revue Roumaine. Chem.* 18 (1973) 1367.
- [15] R.W. Meschke and W.H. Hartung, *J. Org. Chem.* 25 (1960) 137.
- [16] M.A. Aramendia, V. Borau, C. Jimenez, J.M. Marinas, M.E. Sempere and P. Urbano, *Appl. Catal.* 43 (1988) 41.
- [17] M.A. Aramendia, V. Borau, J.F. Gomez, A. Herrera, C. Jimenez and J.M. Marinas, *J. Catal.* 140 (1993) 335.
- [18] Ch-Sh. Chen and H-W. Chen, *J. Chem. Soc., Faraday Trans.* 92 (1996) 1595.
- [19] P. Tundo, S. Zinovyev and A. Perosa, *J. Catal.* 196 (2000) 330.
- [20] B. Corain and M. Kralik, *J. Mol. Catal. A* 159 (2000) 153.
- [21] J. Mol. Catal. A 177 (2001).
- [22] B. Corain, M. Zecca and K. Jerabek, *J. Mol. Catal. A: Chem.* 177 (2001) 3.
- [23] A.K. Zharmagambetova, V.A. Golodov and YU. P. Saltykov, *J. Mol. Catal.* 55 (1989) 406.
- [24] A.K. Zharmagambetova, E.E. Ergozhin, Yu.L. Sheludyakov, S.G. Mukhamedzhanova, I.A. Kurmaanbayeva, B.A. Selenova and B.A. Utkelov, *J. Mol. Catal. A* 177 (2001) 165.
- [25] Z.M. Michalska and K. Strzelec, *Reactive Funct. Polymers* 44 (2000) 189.
- [26] M. Zecca, M. Kralik, M. Boaro, G. Palma, S. Lora, M. Zancato and B. Corain, *J. Mol. Catal. A: Gen.* 129 (1998) 27.
- [27] A. Biffis, B. Corain, Z. Cvengrosova, M. Hronec, K. Jerabek and M. Kralik, *Appl. Catal. A: Gen.* 124 (1995) 355.
- [28] A. Biffis, B. Corain, Z. Cvengrosova, M. Hronec, K. Jerabek and M. Kralik, *Appl. Catal. A: Gen.* 142 (1996) 327.
- [29] A. Malinauskas, *Synth. Met.* 107 (1999) 75.
- [30] S. Holdcroft and B.L. Funt, *J. Electroanal. Chem.* 240 (1988) 89.
- [31] H. Laborde, J.-M. Leger and C. Lamy, *J. Appl. Electrochem.* 24 (1994) 219.
- [32] E.C. Venancio, W.T. Napporn and A.J. Motheo, *Electrochim. Acta* 47 (2002) 1495.
- [33] S.W. Huang, K.G. Neoh, E.T. Kang, H.S. Han and K.L. Tan, *J. Mater. Chem.* 8 (1998) 1743.
- [34] S.W. Huang, K.G. Neoh, C.W. Shih, D.S. Lim, E.T. Kang, H.S. Han and K.L. Tan, *Synth. Met.* 96 (1998) 117.
- [35] J.W. Sobczak, A. Kosiński, A. Biliński, J. Pielaszek and W. Palczewska, *Adv. Mater. Opt. Electron.* 8 (1998) 295.
- [36] A. Drelinkiewicz and M. Hasik, *J. Mol. Catal. A: Gen.* 177 (2001) 149.
- [37] R.A. Jones (ED.) *Pyrrole, Part I. The Synthesis and the Physical and Chemical Aspects of Pyrrole Ring* (Wiley, New York, 1990).

- [38] M. Hasik, A. Bernasik, A. Drelinkiewicz, K. Kowalski, E. Wenda and J. Camra, *Surf. Sci.* 507–510 (2002) 916.
- [39] A.D. Pomagajło, *Polimernye Immobilizovannyje Metalichesije Katalizatory* (Nauka, Moskwa, 1988) p. 27.
- [40] S. Kumar, R. Verma and S. Gangadharan, *Analyst* 118 (1993) 1085.
- [41] Y.C. Liu and B.J. Hwang, *Thin Solid Films* 339 (1999) 233.
- [42] N. Cioffi, L. Torsi, L. Sabbatini, P.G. Zamboni and T. Bleve-Zacheo, *J. Electroanal. Chem.* 488 (2000) 42.
- [43] R.J. Gorte, *J. Catal.* 75 (1982) 164.
- [44] P. Chou and M.A. Vannice, *J. Catal.* 104 (1987) 1.
- [45] R.J. Madon, J.P. O'Connell and M. Boudart, *AIChE J.* 24 (1978) 904.
- [46] Landolt-Bornstein, *Zahlenwerte und Funktionen aus Physik-Chemie-Astronomie-Geophysik und Technik*, sechste auflage, Band II, Teil 2 (Springer-Verlag, Berlin, Göttinger, Heidelberg), 1962.
- [47] R.J. Madon and M. Boudart, *Ind. Eng. Chem. Fundam.* 21 (1982) 438.
- [48] P. Dannelun, M. Boman, S. Slafstrom, R. Salaneck, R. Lazzaroni, C. Fredriksson, J. Bredas, R. Zamboni and C. Taliani, *J. Chem. Phys.* 99 (1993) 664.
- [49] A. Lachkar, A. Selmani and E. Sacher, *Synth. Met.* 72 (1995) 73.
- [50] A. Lachkar, A. Selmani, E. Sacher, M. Leclerc and R. Mokhliss, *Synth. Met.* 66 (1994) 209.